# The low-redshift 3CRR galaxies

Mark Birkinshaw

University of Bristol

# Outline

1. The low-z 3CRR project
2. X-ray imaging – some examples
3. Statistics
4. Physical processes: generalizations

# 1. The low-*z* 3CRR project

- Low-*z* 3CRR galaxies are a well-selected set of active galaxies, with only minor orientation bias
- $z < 0.1$, 1 arcsec < 2 kpc; sub-galaxy scales resolved by *Chandra*
- Should have good s/n for detection of gas/radio interactions
- Wide range of structures: starburst (M 82), FR I (***all*** the 3CRR FR I, e.g., 3C 31), FR I/II (e.g., NGC 6251), FR II (e.g., 3C 98)
- Wide range of galaxy and gas environments: rich clusters (e.g., 3C 84), groups, relatively isolated (usually with companions)
- Wide range of optical spectral types

# 1. The low-*z* 3CRR project

Try to assemble complete set to $z = 0.1$to avoid biases in physics inference.

Problems:

- The objects still to be observed are usually less exciting, which made it hard to persuade TACs to award time
- The current telescope suite isn't sufficiently well matched for the studies to be simple (and the best are non-STFC …)
- Range of integration times means uniformity of feature detection is compromised.

Complete set of Chandra (and Spitzer) images in hand, following large project in AO11 and wrap-up observation in AO12.

# 1. The low-*z* 3CRR project

Both sub-projects

Mark Birkinshaw, Diana Worrall

Chandra project (+HST add-on)

Dan Evans, Eric Perlman, Martin Hardcastle, Ralph Kraft, Liz Mannering

Spitzer project

Peter Barthel, Paul Green, Dean Hines, Eric Hooper, Charles Lawrence, Ilse van Bemmel, Belinda Wilkes, Steve Willner, Amelia Bliss

# 1. The low-z 3CRR project

The full sample contains 36 objects, of which 35 are “genuine” radio galaxies.

**All** that were previously looked at have interesting X-ray structure when observed with *Chandra*.

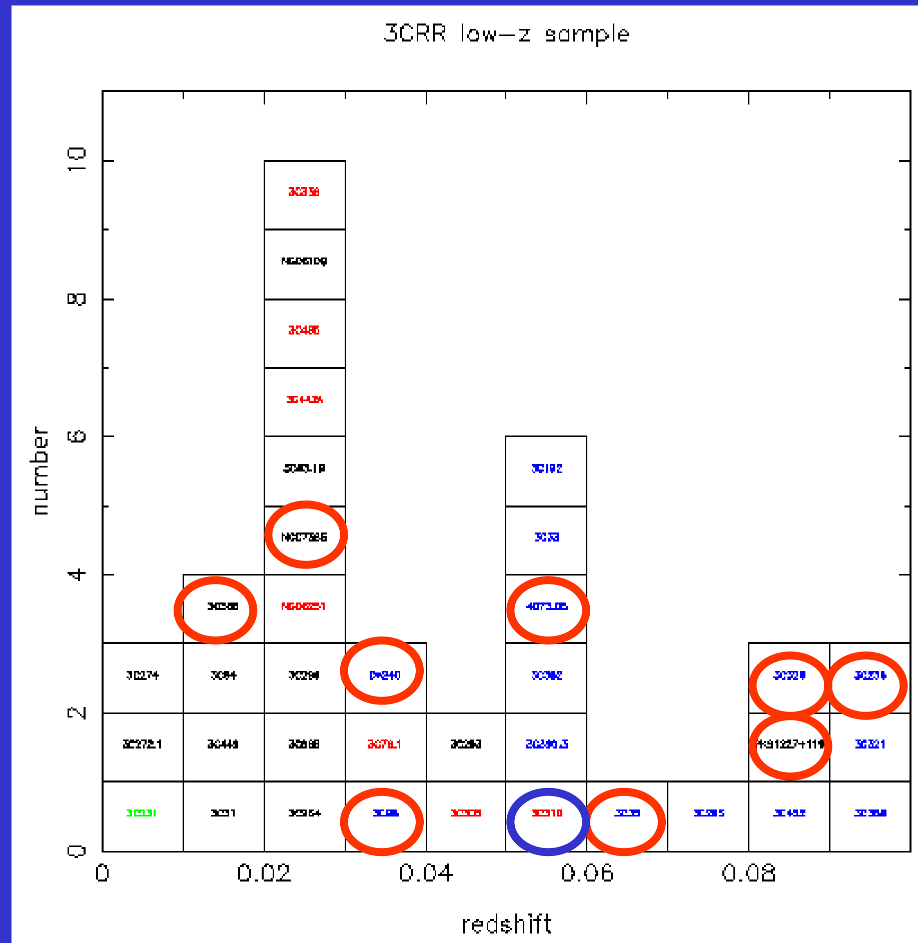

# 2. X-ray imaging: new data

The 3C 35 image from *Chandra* ACIS-I.

Shortest exposure (25 ks).

0.5-2.5 keV

Not very inspiring: hence problem with TACs.

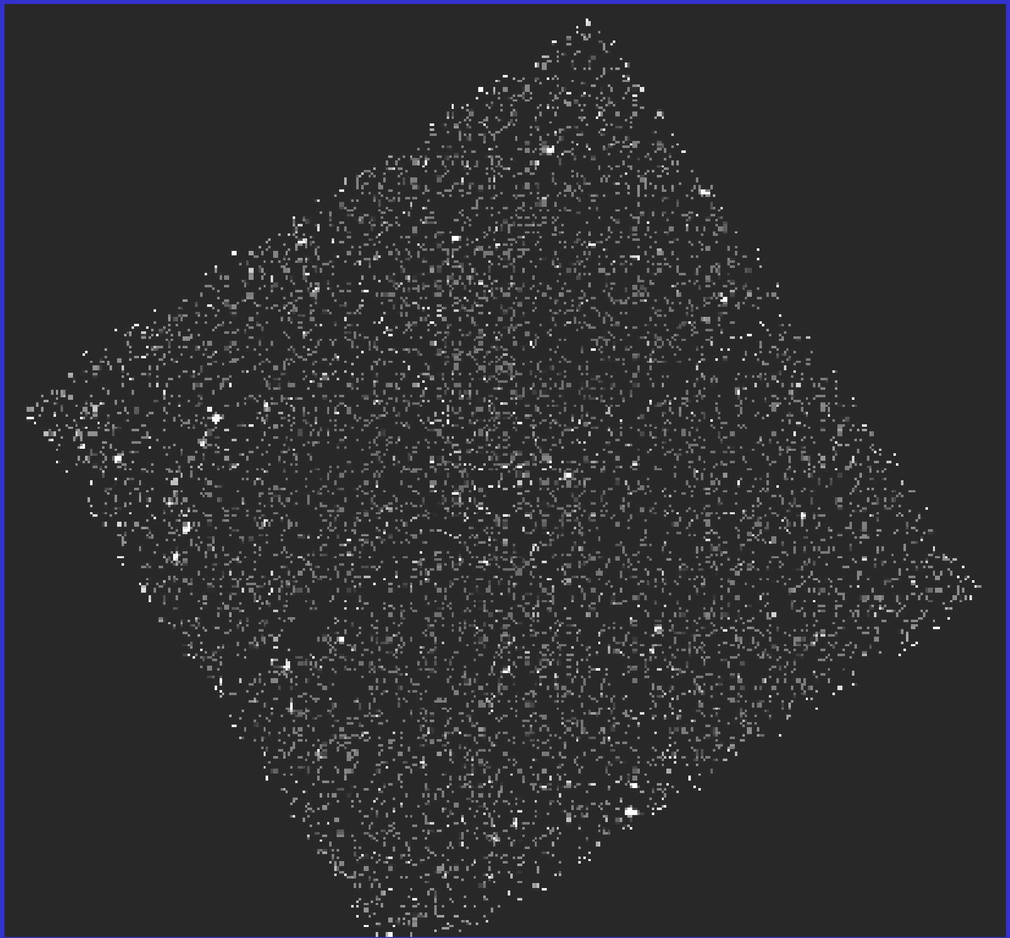

# 2. X-ray imaging: new data

3C 35, after smoothing.

X-rays brighter under the lobes: inverse-Compton emission.

Central gas “belt”, but no obvious external atmosphere.

No detected X-ray hot spot.

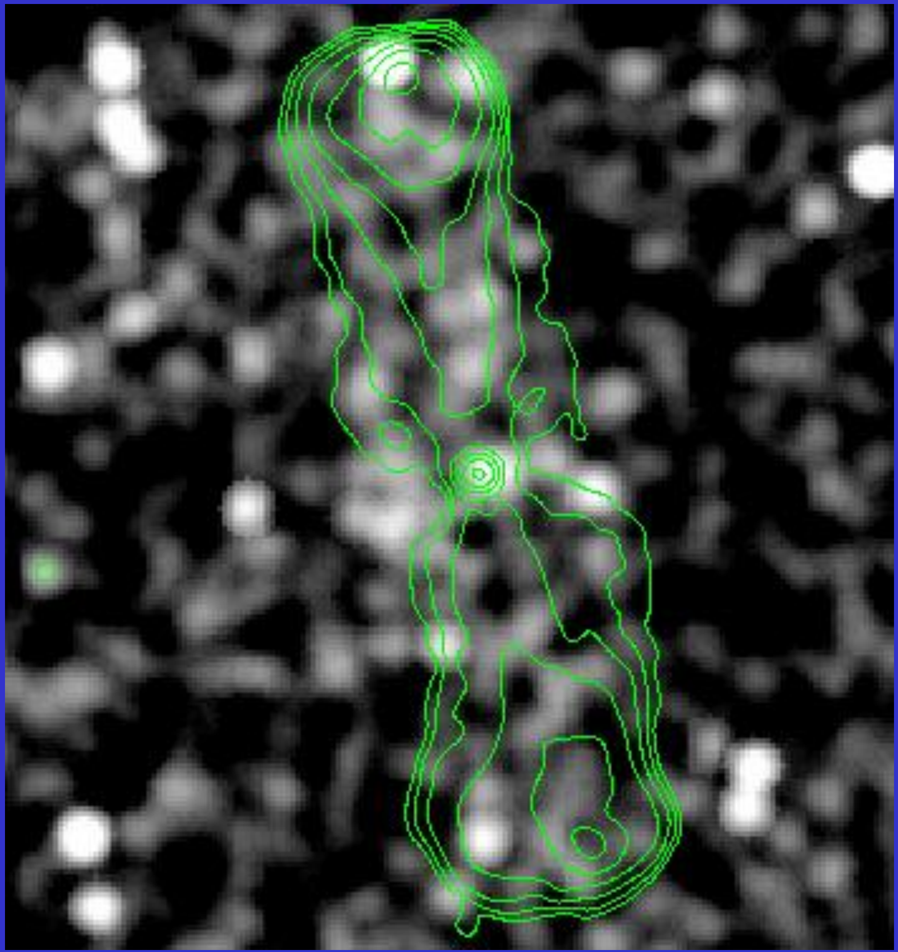

# 2. X-ray imaging: new data

3C 386
Chandra 0.5-2.5 keV
greyscale; smoothed.
VLA B array contours.
~ 4 arcsec resolution.

Core; gas belt; iC from lobe (?)

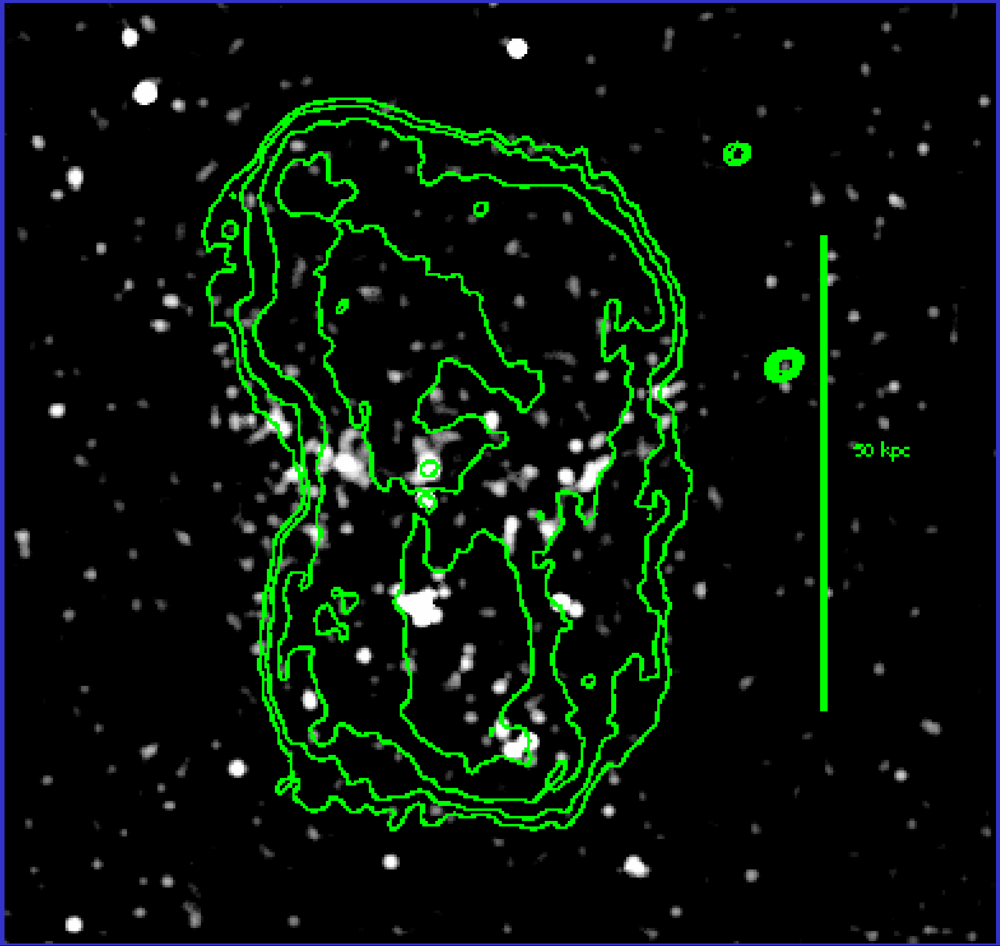

# 2. X-ray imaging: new data

NGC 7385
Chandra 0.5-2.5 keV greyscale.
VLA L-band/C-band contours.
[Also HST jet]

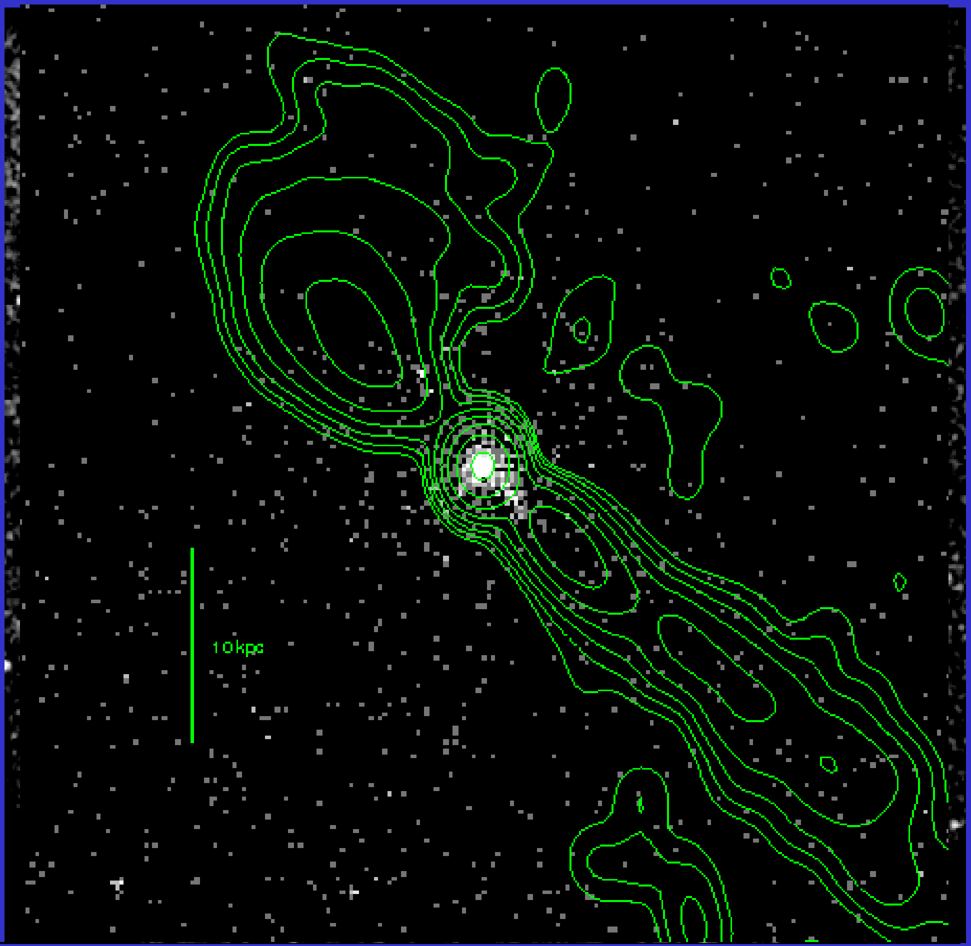

# 2. X-ray imaging: new data

3C 98
Chandra 0.5-2.5 keV greyscale.
VLA A array contours.
~ 1 arcsec resolution.

Central gas belt; gas pushing on lobe to N; some emission on “jet ridge”

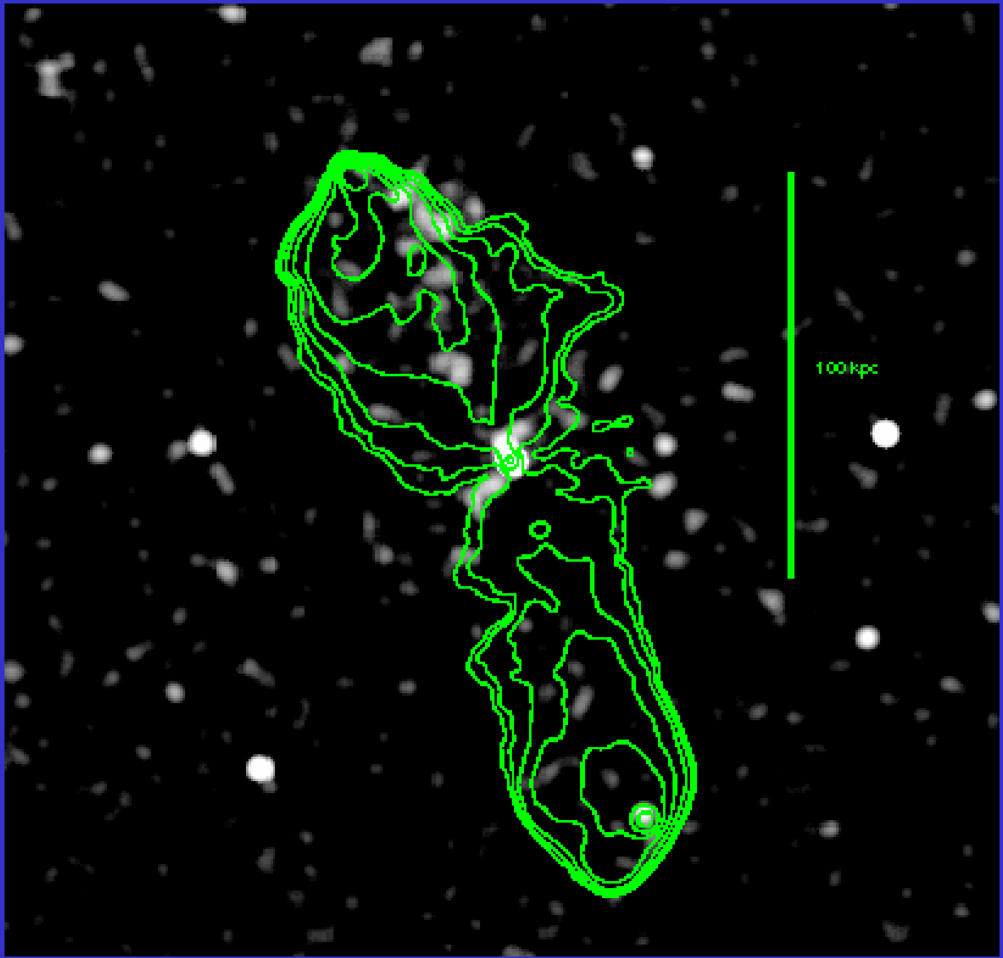

# 2. X-ray imaging: new data

DA 240
Chandra 0.5-2.5 keV greyscale.

VLA contours.
~ 4 arcsec resolution.

iC emission; core; hotspot; some exterior gas?

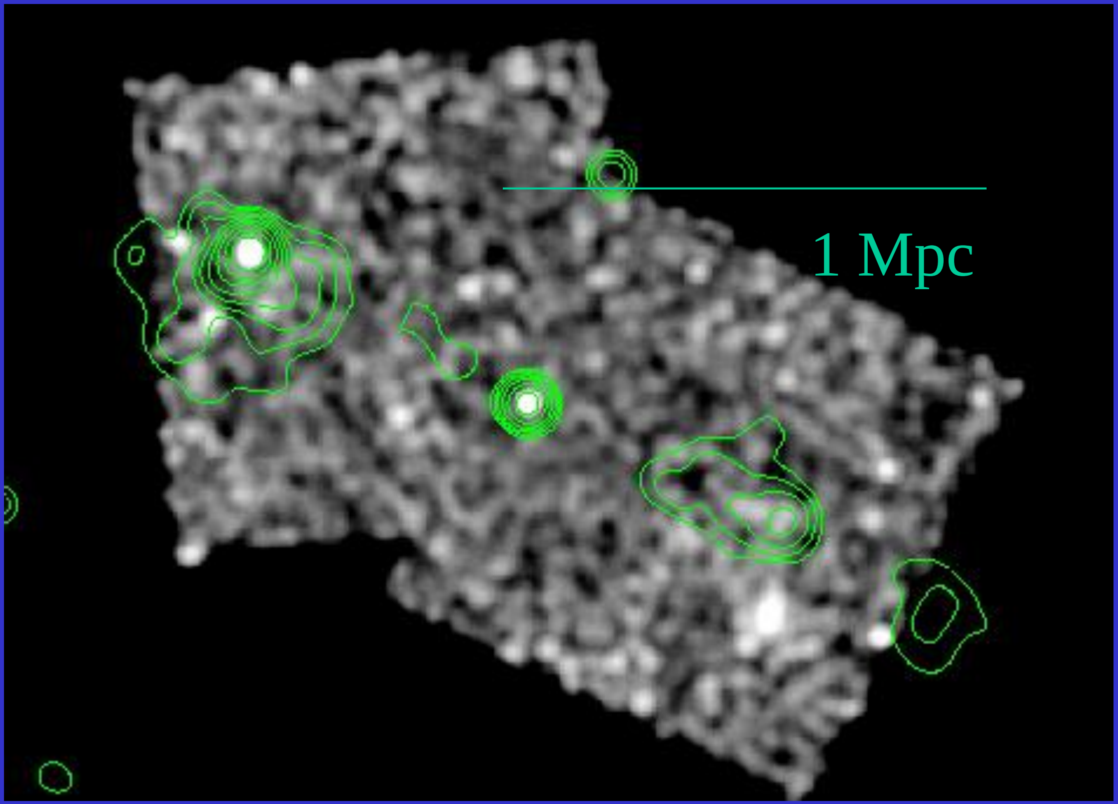

# 2. X-ray imaging: new data

4C 73.08
Chandra 0.5-2.5 keV
greyscale.

Faint emission from W
hot spot.

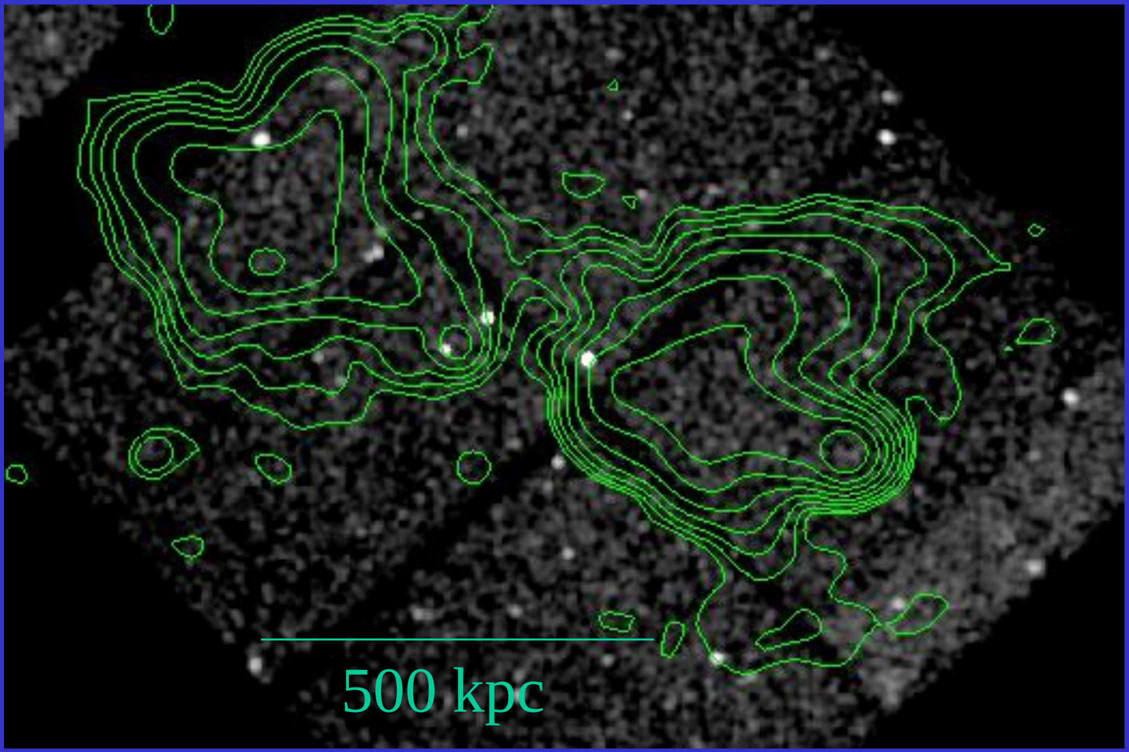

# 2. X-ray imaging: new data

PKS 1227+119
Chandra 0.5-2.5 keV greyscale.
VLA B array, L-band contours.
~ 0.5 arcsec resolution.

Large-scale structure not shown.

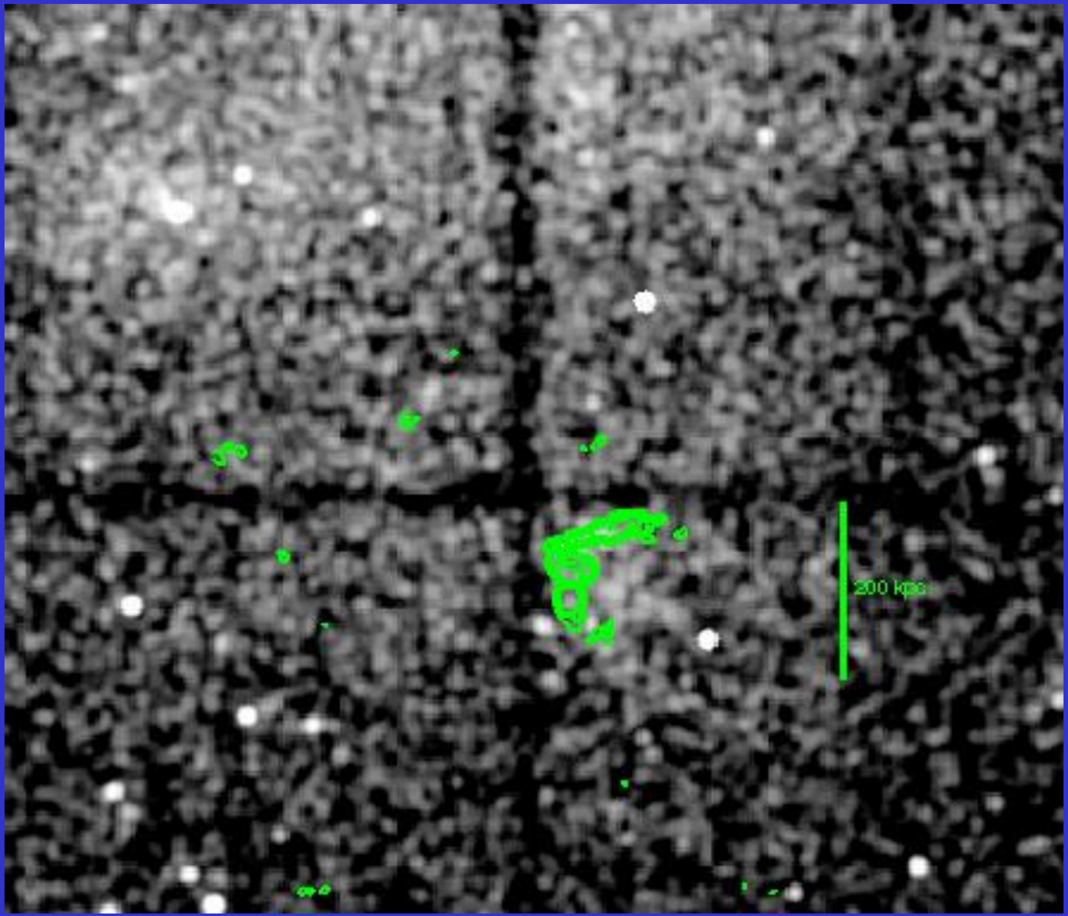

# 2. X-ray imaging: new data

3C 326
Chandra 0.5-2.5 keV greyscale.
NVSS contours.
4 arcsec resolution X-ray.

Inverse-Compton emission from one part of one lobe.

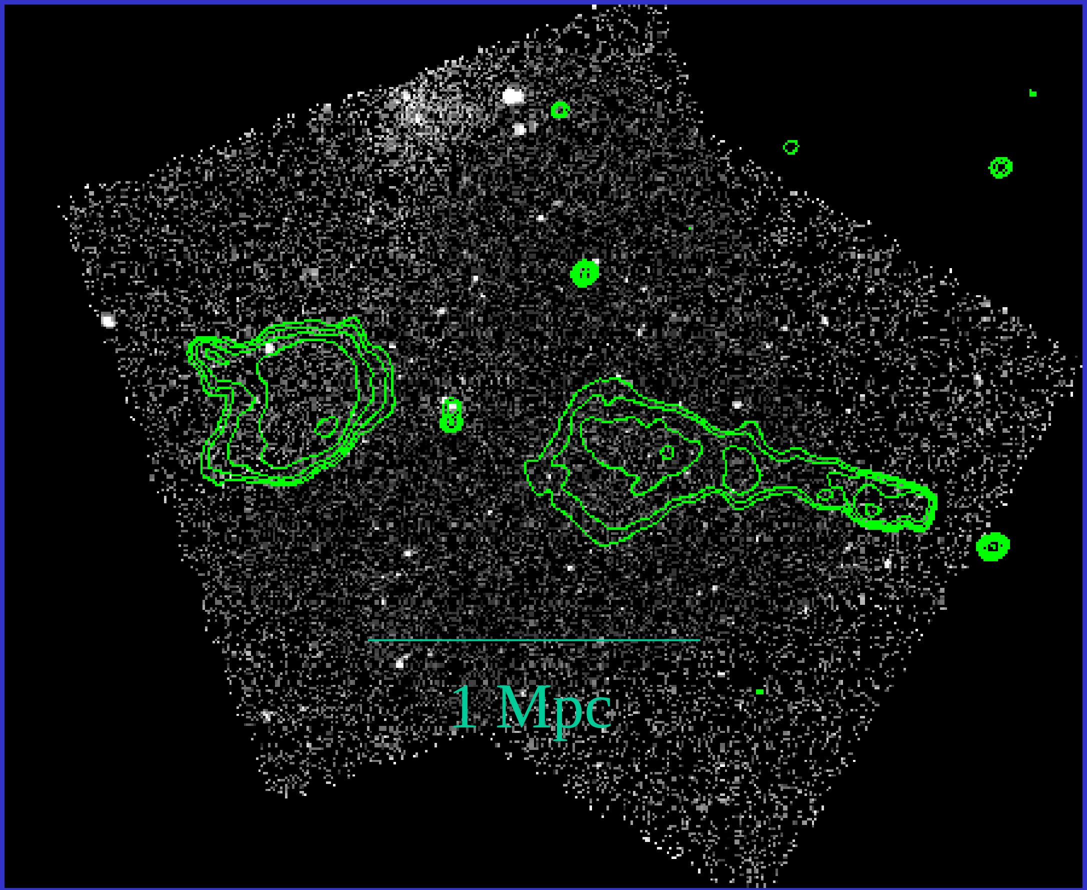

# 2. X-ray imaging: new data

3C 236
Chandra 0.5-2.5 keV greyscale (smoothed).

Inverse-Compton emission and hot spots.

No obvious gas.

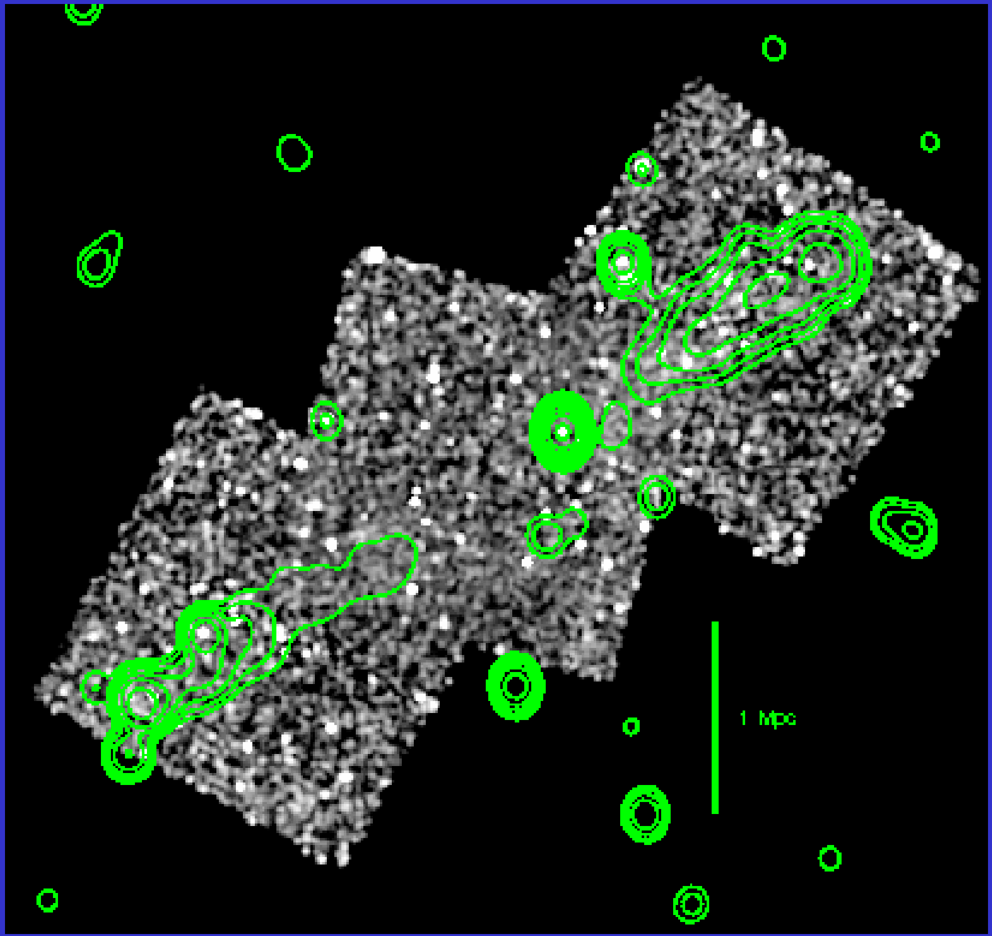

# 2. X-ray imaging: new data

3C 310
Chandra 0.5-2.5 keV
greyscale (smoothed).

Large-scale
atmosphere, with
central cavity, outer
sharp edge, etc.

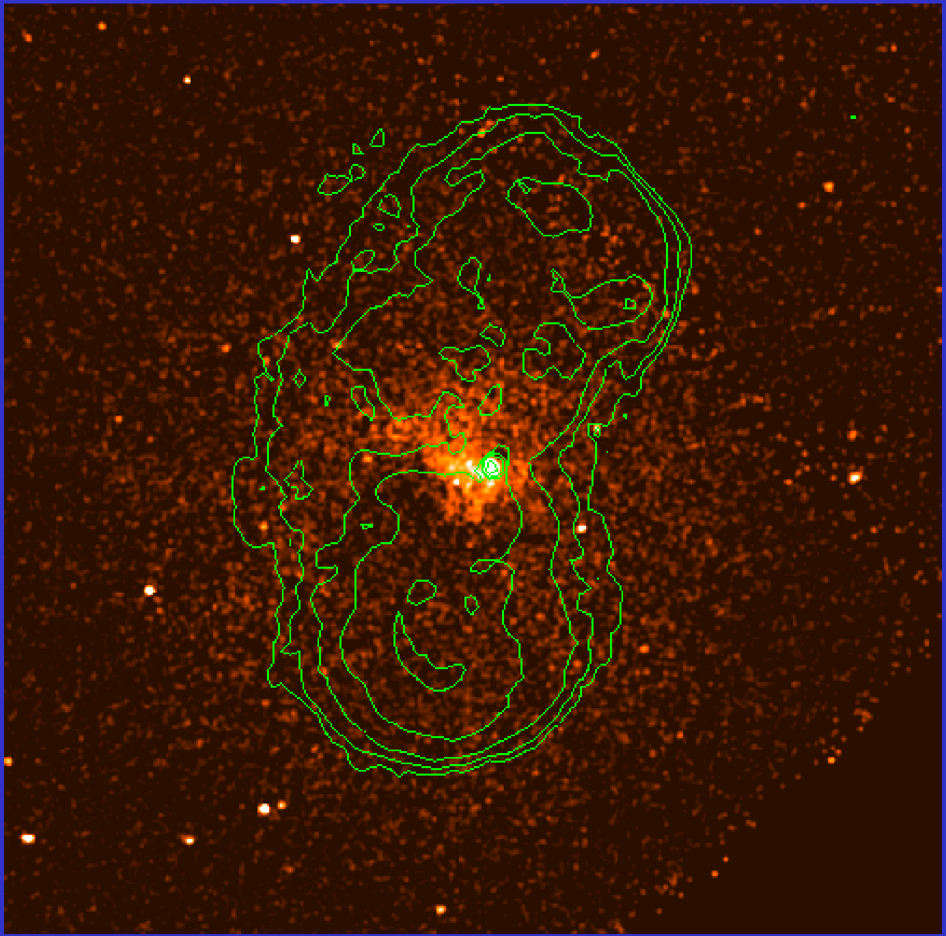

# 3. Statistics

| | FR I | FR I/II | FR II | *n* |
|---|---|---|---|---|
| low $P_{178}$ | 8 | 3 | 0 | 11 |
| med $P_{178}$ | 4 | 4 | 4 | 12 |
| high $P_{178}$ | 2 | 0 | 10 | 12 |
| *n* | 14 | 7 | 14 | |

No surprises: power and FR type closely related

# 3. Statistics

| | X-ray hot spot/s | No hot spots | *n* |
|---|---|---|---|
| low $P_{178}$ | 0 | 11 | 11 |
| med $P_{178}$ | 4 | 8 | 12 |
| high $P_{178}$ | 9 | 3 | 12 |
| *n* | 12 | 23 | |

Essentially same as FR class, except that X-rays aren't always seen from radio hot spots in shorter exposures

# 3. Statistics

| | X-ray jet | No X-ray jet | *n* |
|---|---|---|---|
| low $P_{178}$ | 7 | 4 | 11 |
| med $P_{178}$ | 8 | 4 | 12 |
| high $P_{178}$ | 3 | 9 | 12 |
| *n* | 18 | 17 | |

High power → low jet detection probability

But jets short and faint, so harder to see at high *z*

Reverses at highest (quasar) powers: mechanism change

# 3. Statistics

| | Cluster gas | No cluster gas | *n* |
|---|---|---|---|
| low $P_{178}$ | 7 | 4 | 11 |
| med $P_{178}$ | 5 | 7 | 12 |
| high $P_{178}$ | 4 | 8 | 12 |
| *n* | 16 | 19 | |

High power → low gas detection probability
Caveat: exposure times not entirely consistent.

# 3. Statistics

| | Cluster or group gas | No gas detected | *n* |
|---|---|---|---|
| Cluster env | 13 | 4 | 17 |
| Group env | 3 | 7 | 10 |
| Field | 0 | 9 | 9 |
| *n* | 16 | 20 | |

Comforting that galaxy and X-ray definitions of environment mostly agree!

# 3. Statistics

| | Cavity/ies | No cavity | *n* |
|---|---|---|---|
| low $P_{178}$ | 4 | 7 | 11 |
| med $P_{178}$ | 5 | 7 | 12 |
| high $P_{178}$ | 3 | 9 | 12 |
| *n* | 12 | 23 | |

High power → low cavity detection probability
But high-power sources larger, so harder to see at high *z*
Probability of seeing cavity ~ 100% if clear gas

# 3. Statistics

| | Belt | No belt | $n$ |
|---|---|---|---|
| low $P_{178}$ | 6 | 5 | 11 |
| med $P_{178}$ | 5 | 7 | 12 |
| high $P_{178}$ | 8 | 4 | 12 |
| $n$ | 19 | 16 | |

Some selection effect against detection at high *z*.
But belts seem common, and may always be present.

# 3. Statistics

| | iC lobes | No iC | *n* |
|---|---|---|---|
| low $P_{178}$ | 0 | 11 | 11 |
| med $P_{178}$ | 3 | 9 | 12 |
| high $P_{178}$ | 6 | 6 | 12 |
| *n* | 12 | 23 | |

High power → more inverse-Compton power
Mostly FR-II property. Electrons well confined to lobes.

# 4. Physical processes: generalizations

- X-ray jets are common in FR I radio sources – in every deep-enough exposure we see jets.
- FRI jets are synchrotron from radio to X-ray; fields ~ 15 nT, X-ray emitting electron lifetimes ~ 30 yr, broken power law spectra with $E_{break}$ ~ 300 GeV.
- X-ray jets are more one-sided than the radio jets: faster flows.
- Get offsets between radio and X-ray peaks of jet brightness lumps.

- Radio lobes are faint inverse-Compton emitters, and show the plasma is near equipartition.
- Questions to do with the confinement of the radio lobes become worse with giants like DA240, 3C236, with little/no gas nearby.

# 4. Physical processes: generalizations

- Hot spots not dominant in low-*z* sample, and absent in low-power objects.
- Appearance of some emission at heads of highest-*z* objects at level consistent with earlier work on higher-*z* sample (Hardcastle *et al*.) – inverse-Compton plus synchrotron emission.
- Small offsets in hot spot position between X-ray and radio peaks: X-ray closer to core, so association with end of jet rather than hot-spot itself?

# 4. Physical processes: generalizations

- Lobe inverse-Compton emission consistent with modest particle domination over minimum energy (Croston *et al*.).
- In many cases the minimum-energy internal pressures are lower than the external pressures from surrounding gas – survival of lobes requires unseen pressure source.
- In giants, scales of lobes far larger than scales of likely atmospheres: what confines the lobes?
- Structure of narrow lobes a particular issue: e.g., 3C 236, 3C 326 west.
- Lobes clearly lifting and compressing gas, even in poor environments – the 3C 98 notch is a particularly good example.
- In some cases the gas is shifting the lobes – e.g., in 3C 442A (Worrall *et al*. 2007): energy exchange is a two-way process.